Vol. No.6, Issue No. 01, January 2017 www.ijarse.com



# Enhanced orange-red emission from alkaline earth metal oxide doped with Sm<sup>3+</sup> and co-doped with some alkali metal ions

Subhash Chand<sup>1</sup>, Jaibir S Yadav<sup>2</sup>, Ishwar Singh<sup>3</sup>

<sup>1</sup>Department of Chemistry, Maharshi Dayanand University, Rohtak, Haryana (India)

<sup>2</sup>Department of Chemistry, A.I. Jat H.M. College, Rohtak, Haryana (India)

<sup>3</sup>Pro-Vice Chancellor, PDM University, Bahadurgarh, Haryana (India)

#### **ABSTRACT**

CaO:Sm<sup>3+</sup>,M<sup>+</sup> (Li<sup>+</sup>, Na<sup>+</sup>, K<sup>+</sup>), SrO:Sm<sup>3+</sup> and CaSrO<sub>2</sub>:Sm<sup>3+</sup> nano-phophors were prepared by combustion synthesis method and the samples were further heated to ~1000 °C to improve the crystallinity of the materials. The structure and morphology of materials were examined by X-ray diffraction and scanning electron microscopy. The morphology of CaO:Sm<sup>3+</sup> and co-doped with alkali metal ions powders was very similar. Small and coagulated particles of nearly cubical shapes with small size distribution having smooth and regular surface were formed. The surface morphology of SrO and CaSrO<sub>2</sub> materials was not smooth and coagulated particles of irregular shapes with different sizes were observed. Under the excitation of UV light (245nm) and low-voltage electron beams (1-3kV), this nano-phophors show the characteristic emissions of phosphor consist of five emission peaks, which are attributed to the transitions from  ${}^4G_{5/2}$  state to  ${}^6H_J$  (J=5/2, 7/2, 9/2, 11/2,13/2) states of Sm<sup>3+</sup> ions with Orange, Orange-red and red color with emission peaks located at 570, 592, 610, 654, 705 nm respectively. Among these emission peaks, the transition emission  ${}^4G_{5/2} \rightarrow {}^6H_J(J=5/2, 7/2, 9/2)$  for peak at 570, 592, 610 nm is strongest for Orange, Orange-red and strong for Red emission respectively due to the magnetic dipole transition of Sm<sup>3+</sup> ion having a magnetic dipole (MD) allowed one and also an electric dipole (ED) dominated one but the other weak transition like  ${}^4G_{5/2} \rightarrow {}^6H_{11/2} & {}^4G_{5/2} \rightarrow {}^6H_{13/2}$  (654 nm, 705 nm red) is purely an ED one. Photoluminescence followed the order as in CaO > CaSrO<sub>2</sub> > SrO lattices. A remarkable increase of photoluminescence intensity was observed by the co-doping of alkali metal ions particularly  $K^+$  ions in  $CaO:Sm^{3+}$ .

**Keywords:**  $CaO:Sm^{3+}, M^{+}(Li^{+}, Na^{+}, K^{+});$   $SrO:Sm^{3+};$   $CaSrO_{2}:Sm^{3+};$  Combustion synthesis; Photoluminescence, Magnetic dipole, Electric dipole.

#### I. INTRODUCTION

The synthesis of inorganic phosphor materials with varied morphology and texture, controlled crystallography, and micro- or nano-scale architectures are important goals because of their novel chemical, physical and optical properties [1-3]. Very recently, many rare-earth-doped optical materials such as titanates, silicates, oxides and borates with different uniform shapes have been obtained from different processes like sol gel, co-precipitation and modified solid state methods [4-7]. These materials find their applications in lighting, information display,

Vol. No.6, Issue No. 01, January 2017

## www.ijarse.com



and optoelectronics technology. Eu<sup>3+</sup> ion is an especially important activator for red phosphors which has been extensively studied for years [8, 9], because the visible emission of Eu<sup>3+</sup> ion in 4f shell is insensitive to the influence of the surroundings due to the shielding effect of 5s, 5p electron [10]. More recently, the alkaline earth oxides as hosts for trivalent europium ions, which substitute alkaline earth ions readily into the lattice, exert further interest in their fundamental properties and seem to be a good potential choice for the field emission display (FED) red phosphor [11]. The CaO:Sm<sup>3+</sup>, SrO: Sm<sup>3+</sup> and their mixed oxides like CaSrO<sub>2</sub>:Sm<sup>3+</sup> and same lattices doped with Eu<sup>3+</sup> are expected to act as one of the most promising orange-red luminescent materials [12]. It has been pointed out that when a trivalent metallic ion is incorporated into a host lattice and substitutes for divalent metallic ion, the charge is unbalance, which has an effect on luminescence intensity. Hence in order to enhance the luminescence intensity, alkali metals ions should be co-doped in the host. When these materials are synthesized through the traditional high-temperature solid-state method, the product is mostly found to be either of irregular morphology or agglomerate with serious reunion and high hardness, which affects the luminescence efficiency of the phosphors during the later milling. As we know different material preparation methods have some important effects on material microstructure and physical properties. The combustion synthesis provides an interesting alternative over other elaborated techniques because it offers several attractive advantages such as: simplicity of experimental set-up; surprisingly short time between the preparation of reactants and the availability of the final product; and being cheap due to energy saving. The main advantage of this method is the rapid decomposition of the rare earth nitrate in the presence of an organic fuel. During the reaction, many gases, such as CO<sub>2</sub>, N<sub>2</sub>, NO<sub>2</sub> and H<sub>2</sub>O, as well as a large amount of heat are released in a short period of time before the process terminates with white, foamy and crisp products. Many times final products are found to be composed of nano-sized particles. This work has been carried out with the aim to prepare and compare the high intensity photoluminescence nano-sized crystalline powders of CaO, SrO and their mixed oxides CaSrO2 doped with Sm<sup>3+</sup> after sintering at 1000°C. The effect of monovalent alkali ions (Li<sup>+</sup>, Na<sup>+</sup>, K<sup>+</sup>) into CaO:Sm<sup>3+</sup> to enhance the luminescence intensity and the possible mechanism has been proposed. The crystalline structure and morphology of prepared materials have also been discussed. The crystalline structure of prepared materials, morphology of particles and their photoluminescence properties are characterized by XRD, SEM and emission spectra with 245 nm laser for excitation.

#### II. EXPERIMENTAL

High purity [Ca(NO<sub>3</sub>)<sub>2</sub>], [Sr(NO<sub>3</sub>)<sub>2</sub>], [Sm(NO<sub>3</sub>)<sub>3</sub>], NaNO<sub>3</sub>, KNO<sub>3</sub>, LiNO<sub>3</sub> and urea [H<sub>2</sub>NCONH<sub>2</sub>] from Aldrich chemicals were purchased as starting materials. Sm<sup>3+</sup> doped and M<sup>+</sup> co-doped (M<sup>+</sup> = Li, Na, K) nanocrystals with formula 1-xCaO:xSm<sup>3+</sup>;M<sup>+</sup>, 1-xSrO:xSm<sup>3+</sup> and 1-xCaSrO<sub>2</sub>:xSm<sup>3+</sup> and where x is 1mole%, were prepared by heating rapidly an aqueous concentrated paste containing a calculated amount of metal nitrates and urea in a preheated furnace maintained at 500 °C. Urea was used as a fuel and its amount was calculated using total oxidizing and reducing valencies [13]. In such cases, the material undergoes rapid dehydration and foaming followed by decomposition, generating combustible gases. These volatile combustible gases ignite and burn with a flame, yielding a voluminous solid. In the present case, the combustion process utilized the enthalpy of combustion for the formation and the solid obtained was again fired at 1000 °C for 3 h to increase the brightness and crystallinity.

Vol. No.6, Issue No. 01, January 2017

## www.ijarse.com



The morphology of the crystals was studied by scanning electron microscopy (SEM) using JEOL JSM6300 scanning electron microscope operating at 10 kV. Photoluminescence (PL) experiments were performed in backscattering geometry using a He–Cd laser (245 nm) with an optical power of 30 mW for excitation. The emitted light was analyzed by HR-4000 Ocean Optics USB spectrometer optimized for the UV–vis range. For the photoluminescence measurement, 0.05 g powder samples were pressed into pellets (10 mm diameter and 1 mm thickness) and then exposed to a UV lamp at 245 nm. All measurements were carried out at room temperature. The structural characterization was performed by high resolution X-ray diffraction (XRD) using Rigaku Ultima IV diffractometer in the  $\theta$ –2 $\theta$  configuration and using Cu K $\alpha$  radiation (1.541841 Å).

#### III. RESULTS AND DISCUSSION

X-Ray diffraction patterns were used to examine the crystal structure and phase purity of the products, and the typical XRD patterns of Sm<sup>3+</sup> doped CaO and SrO and CaSrO<sub>2</sub> samples and Sm<sup>3+</sup> co-doped with Li<sup>+</sup> or Na<sup>+</sup> or K<sup>+</sup> in CaO are shown in Fig.1a,b respectively. It may be observed that in XRD pattern corresponding to CaO:Sm<sup>3+</sup> in Fig.1a, the most of the diffraction peaks are assigned to face-centered cubic crystalline phase of calcium oxide (no. JCPDS 37-1497) with space group Fm-3m and there is another phase present corresponding to CaO4 (no. JCPDS 21-0155). No any other impurity phase was detected, indicating that the doped ions were occupied the Ca<sup>2+</sup> sties. Almost identical patterns are obtained in fig 1b. This indicates the co-doping of alkali metal ions with Sm<sup>3+</sup> do not effect significantly the structure of CaO. As the ionic radius of Sm<sup>3+</sup> and Na<sup>+</sup> are 94.7and 102 nm (coordination number = 6) are not much different from that of Ca<sup>2+</sup> (100 nm, coordination number = 6). These ions are likely to substitute for  $Ca^{2+}$  ion and acts as the luminescence center [10]. However, the other ions like Li<sup>+</sup> and K<sup>+</sup> have ionic radii 76 and 138 nm respectively with a large difference, are also incorporated in CaO lattice successfully. Due to this difference of ionic radii of Li<sup>+</sup> and K<sup>+</sup>, the CaO lattice had slight deformations which lead to the variation in the heights of diffraction peaks in their patterns. In Fig.1a the XRD graph for Sm<sup>3+</sup> doped SrO material is shown. There are mainly two phases of SrO<sub>3</sub>(no. JCPDS 001-1113) and Sm<sub>2</sub>O<sub>3</sub>(JCPDS Card No. 15-0813) present in this phosphor. The XRD patterns of mixed CaSrO<sub>2</sub> and doped with Sm<sup>3+</sup> show the presence of three phases of CaO<sub>4</sub> (no. JCPDS 21-0155), SrO<sub>2</sub> (no. JCPDS 001-1113) and Sm<sub>2</sub>O<sub>3</sub> (JCPDS Card No. 15-0813). The presence of separate Sm<sub>2</sub>O<sub>3</sub> phase in SrO:Sm<sup>3+</sup> and CaSrO<sub>2</sub>:Sm<sup>3+</sup> phosphors also show the incorporation of Sm<sup>3+</sup> ions in these host lattices, but not complete.

Effect of the incorporation of  $\operatorname{Li}^+$ ,  $\operatorname{Na}^+$  and  $\operatorname{K}^+$  ions on CaO:  $\operatorname{Sm}^{3+}$  structure had been investigated to study the photoluminescent behavior of this lattice.  $\operatorname{Li}^+$ ,  $\operatorname{Na}^+$  and  $\operatorname{K}^+$  ions occupied the position of  $\operatorname{Ca}^{2+}$  site. As the ionic radius of  $\operatorname{Li}^+$  ion is less, there is a possibility of some of the ions to reside in interstitial sites between or among the host ions. For  $\operatorname{Na}^+$  ions, they could be located at  $\operatorname{Ca}^{2+}$  sites more easily than for  $\operatorname{K}^+$  ions because of their bigger ionic radii. In Fig.1b, note that the representative diffraction data of CaO:  $\operatorname{Sm}^{3+}$  material doped with  $\operatorname{Li}^+$ ,  $\operatorname{Na}^+$ ,  $\operatorname{K}^+$  ions were obviously almost identical but the relative intensities of crystal faces (111), (200) and (221) were different from each other. We think this observation can be assigned to the enormous changes in lattice constants of these samples. The corresponding unit-cell constants and unit cell volumes of cubic  $\operatorname{CaO}:\operatorname{Sm}^{3+}$  samples as well as doped with  $\operatorname{Li}^+$ ,  $\operatorname{Na}^+$ ,  $\operatorname{K}^+$  are calculated from the distance between the adjacent (200) planes corresponding to direction peaks near  $2\theta = 37.30$  and are listed in Table 1.

Vol. No.6, Issue No. 01, January 2017

www.ijarse.com



Table 1. The calculated lattice parameters of CaO:Sm<sup>3+</sup> doped with Li<sup>+</sup>, Na<sup>+</sup>, K<sup>+</sup>

Phosphors	2θ	hkl/200	a (A)	V (A <sup>3</sup> )
CaO:Sm <sup>3+</sup>	37.340	2.4062	4.8122	111.435
CaO:Sm <sup>3+</sup> ,Li <sup>+</sup>	37.282	2.4098	4.8197	111.967
CaO:Sm <sup>3+</sup> ,Na <sup>+</sup>	37.277	2.4103	4.8207	112.015
CaO:Sm <sup>3+</sup> ,K <sup>+</sup>	37.259	2.4115	4.8229	112.177

It is obvious that if the ions with larger radius substitute the smaller cations in the crystalline lattice, the cell volume of the host compound is increased [13,14]. Therefore, as shown in Table 1, the cell volumes of CaO:Sm<sup>3+</sup>,Na<sup>+</sup> and CaO:Sm<sup>3+</sup>,K<sup>+</sup> after doping with Na<sup>+</sup> and K<sup>+</sup> ions increased, because the ionic radii of Na<sup>+</sup> ions (102 pm) and K<sup>+</sup> ions (138pm) are larger than that of Ca<sup>2+</sup> ions (100 pm). The same rule would also apply to CaO:Sm<sup>3+</sup>,Li<sup>+</sup> sample. The cell volume should decrease with the doping of Li<sup>+</sup>. However, the cell volume of CaO:Sm<sup>3+</sup> doped with Li<sup>+</sup> increased, despite the fact that the Li<sup>+</sup> is smaller than Ca<sup>2+</sup>. This increase may be due to the larger size of Li<sup>+</sup> ions than that of interstitial sites.

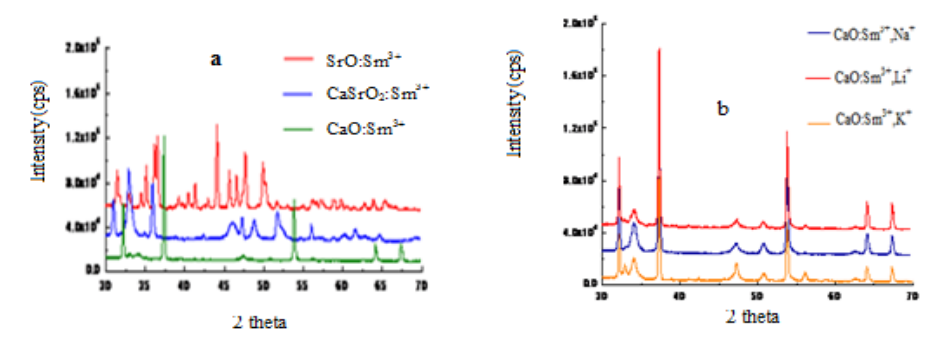


Figure 1. XRD spectra of (a) SrO: Sm<sup>3+</sup>, CaSrO<sub>2</sub>: Sm<sup>3+</sup>, CaO: Sm<sup>3+</sup> and (b) CaO: Sm<sup>3+</sup>, Na<sup>+</sup>, Li<sup>+</sup> & K<sup>+</sup>

#### IV. SEM MICROGRAPHS AND PARTICLE SIZE ANALYSES OF SAMPLES

Crystallinity, particle size, and surface roughness of the phosphor materials have strong effects on the photoluminescence. Fig. 2a,b,c,d exhibits surface morphology of CaO:Sm<sup>3+</sup>; CaO:Sm<sup>3+</sup>,Na<sup>+</sup>; SrO:Sm<sup>3+</sup> and CaSrO<sub>2</sub>:Sm<sup>3+</sup> particles respectively. It is clear from SEM images that the morphology of the sample 2a and 2b are very similar. Small and coagulated particles of nearly cubical shapes with small size distribution having smooth and regular surface may be observed.

Vol. No.6, Issue No. 01, January 2017 www.ijarse.com



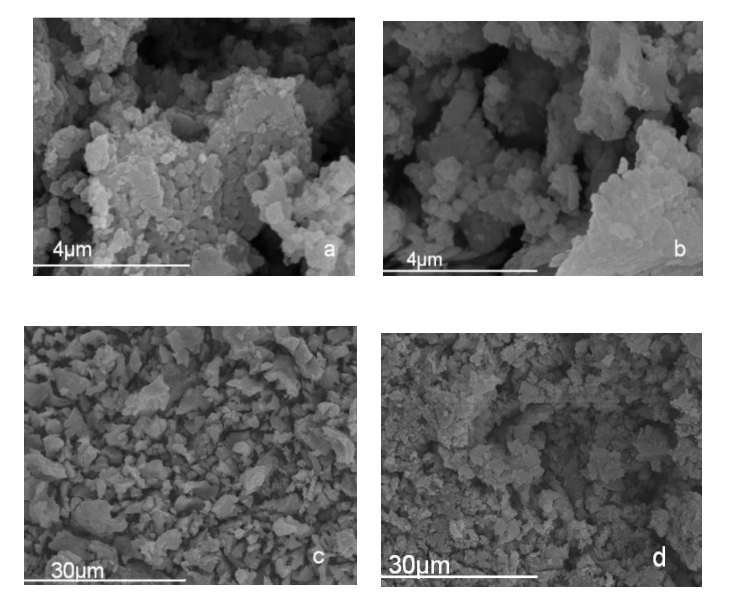


Figure 2. SEM micrographs of (a) CaO:Sm<sup>3+</sup>, (b) CaO:Sm<sup>3+</sup>,Na<sup>+</sup>, (c) SrO:Sm<sup>3+</sup> and (d) CaSrO<sub>2</sub>:Sm<sup>3+</sup>.

The surface morphology of SrO or CaSrO<sub>2</sub> lattices as depicted in Fig. 2c and 2d is not smooth, therefore coagulated particles of irregular shapes with different sizes are observed. The smooth surface of phosphor can reduce the non-radiation and scattering, thus is beneficial to the luminescence efficiency in application [9]. The dense packed small particles can prevent the phosphors from aging.

## V. PHOTOLUMINESCENT PROPERTIES

The room-temperature emission spectra of Sm<sup>3+</sup> doped CaO, SrO and CaSrO<sub>2</sub> crystals and co doped with Li<sup>+</sup>, Na<sup>+</sup> and K<sup>+</sup> in CaO are shown in Fig.3 a,b. The emission spectra were obtained by monitoring an excitation of ultraviolet light at 245 nm and low-voltage electron beams (1-3kV). The obtained products emitted the orangered luminescence of varying intensities, which showed the activator Sm3+ had successfully entered the host lattice of CaO, SrO and CaSrO<sub>2</sub>. The characteristic emissions of Sm<sup>3+</sup> had strong orange-red emission at 570 and 592 nm for  ${}^4G_{5/2} \rightarrow {}^6H_{5/2}$ ,  ${}^4G_{5/2} \rightarrow {}^6H_{7/2}$  transition and strong red emission at 610 nm with  ${}^4G_{5/2} \rightarrow {}^6H_{9/2}$ transition but some other weak transitions observed at 654, 705 nm for  ${}^4G_{52} \rightarrow {}^6H_I$  transitions where J= 11/2,13/2 respectively. The exact positions of emission peaks in various lattices are shown in Table 2. This nano-phophors show the characteristic emissions of phosphor consist of five emission peaks, which are attributed to the transitions from  $^4G_{5/2}$  state to  $^6H_J$  (J=5/2, 7/2, 9/2, 11/2 ,13/2) states of Sm $^{3+}$  ions with Orange , Orange-red and red color. Among these, emission peak located at 570, 592, 610, 654, 705 nm are attributed to the transitions of  ${}^4G_{5/2} \rightarrow {}^6H_{5/2}$ ,  ${}^4G_{5/2} \rightarrow {}^6H_{7/2}$ ,  ${}^4G_{5/2} \rightarrow {}^6H_{9/2}$ ,  ${}^4G_{5/2} \rightarrow {}^6H_{11/2}$  &  ${}^4G_{5/2} \rightarrow {}^6H_{13/2}$  respectively. Among these emission peaks, the transition emission  ${}^4G_{5/2} \rightarrow {}^6H_J(J=5/2, 7/2, 9/2)$  for peak at 570, 592, 610 nm is strongest for Orange, Orange-red and strong for Red emission respectively is due to the magnetic dipole transition of Sm3+ ion having a magnetic dipole (MD) allowed one and also an electric dipole (ED) dominated one but the other weak transition like  ${}^4G_{5/2} \rightarrow {}^6H_{11/2} \& {}^4G_{5/2} \rightarrow {}^6H_{13/2}$  (654 nm, 705 nm red) is purely an ED one. [15, 16]. It is also evident from XRD analysis that CaO samples (doped with  $Sm^{3+}$  and  $Li^+$  or  $Na^+$ ,  $K^+$ ) had the face-centered cubic NaCl structure, which showed that the Sm<sup>3+</sup> ions, occupying the Ca<sup>2+</sup> sites in the CaO lattice, are in sites with

Vol. No.6, Issue No. 01, January 2017

## www.ijarse.com



high symmetric position  $(O_h)$ . On the other hand, the position of  $Sm^{3+}$  in two phases of strontium oxide (SrO and  $Sm_2O_3$ ) may not be at sites of high symmetry, as SrO and  $Sm_2O_3$  belong to tetragonal and monoclinic lattices respectively. Furthermore, we noted that the transition line of  ${}^4G_{5/2} \rightarrow {}^6H_{7/2}$  did not split as was expected for symmetry group  $O_h$ . In these sites, electric dipole transition, such as  ${}^4G_{5/2} \rightarrow {}^6H_{9/2}$ , is forbidden [17]. In accordance to the selection rule, if  $Sm^{3+}$  ion locates in symmetric position, optical transitions between the  ${}^4f_n$  configurations are strictly forbidden. However, lattice vibration of the host lattice CaO reduce the symmetry of  $Sm^{3+}$ , the  ${}^4G_{5/2} \rightarrow {}^6H_{5/2}$  transition would be observed due to the breakdown of the selection rule. The presence of  $CaO_4$  and  $SrO_2$  phases in CaO and SrO lattices respectively are also responsible for reducing symmetric environment around  $Sm^{3+}$ . At the same time, the  $Sm^{3+}$  site must have one symmetry because of non-splitting of  ${}^4G_{5/2} \rightarrow {}^6H_{5/2}$  transition in the fluorescence spectrum. The fact confirms that  $Sm^{3+}$  ions mainly locate in strict symmetric position  $(O_h)$  of the crystal lattice CaO.

Wang and Porter et al [18, 19] explained the emission spectral behavior with three kinds of Sm<sup>3+</sup> or Eu<sup>3+</sup> centres in CaO lattice. The first one, Sm<sup>3+</sup> ion with cubic surroundings; in second centre Sm<sup>3+</sup> ion is on a Ca<sup>2+</sup> site with a calcium vacancy along the (110) direction in the lattice and the third centre had been ascribed to a cluster of Sm<sup>3+</sup> ions. These centers emit orange-red radiations characteristic of Sm<sup>3+</sup> ions. If the emission spectra of Sm<sup>3+</sup> doped CaO, SrO, and CaSrO<sub>2</sub> materials are compared (Fig. 3a), the relative intensities of all emission peaks follow the order CaO >CaSrO<sub>2</sub>>SrO. Low emission intensity of Sm<sup>3+</sup> ions in SrO may be due to lack of efficient energy transfer from Sr<sup>2+</sup> ions to Sm<sup>3+</sup> ions or due to the presence of some surface impurities or surface defects. The smooth morphology and compact packing of CaO:Sm<sup>3+</sup> particles as compared to SrO:Sm<sup>3+</sup> or CaSrO<sub>2</sub>:Sm<sup>3+</sup> particles as depicted in SEM images may be another factor for low intensity values of SrO:Sm<sup>3+</sup> samples. However, the relative positions of all emission peaks in SrO or CaSrO<sub>2</sub> materials remain at the same position as that of CaO:Sm<sup>3+</sup> samples, showing the existence of similar environment for Sm<sup>3+</sup> ions in CaO and SrO lattices.

Table 2. The exact positions of emission peaks in various lattices

Lattices	$^{4}G_{5/2} \rightarrow ^{6}H_{5/2}$	$^{4}G_{5/2} \rightarrow ^{6}H_{5/2}$	$^{4}G_{5/2} \rightarrow ^{6}H_{5/2}$	${}^{4}G_{5/2} \rightarrow {}^{6}H_{5/2}$	$^{4}G_{5/2} \rightarrow ^{6}H_{5/2}$
	(Orange)	(Orange-Red)	(Red)		
CaO:Sm <sup>3+</sup>	570 nm	592 nm	610 nm	654 nm	705 nm
SrO:Sm <sup>3+</sup>	570 nm	587 nm	611 – 621 nm	655 nm	704 nm
CaSrO <sub>2</sub> :Sm <sup>3+</sup>	571 nm	592 nm	611,619,626 nm	655 nm	705 nm
CaO:Sm <sup>3+</sup> , Li <sup>+</sup>	571 nm	593 nm	611,618, 622 nm	654 nm	705 nm
CaO:Sm <sup>3+</sup> ,Na <sup>+</sup>	571 nm	592 nm	611,618,627 nm		705 nm
CaO:Sm <sup>3+</sup> , K <sup>+</sup>	575 nm	591 nm	615 – 624 nm	655 nm	705 nm

Vol. No.6, Issue No. 01, January 2017

www.ijarse.com



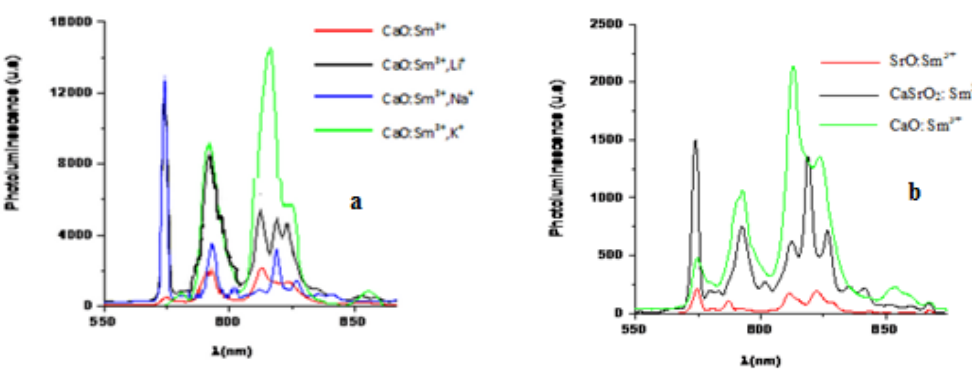


Figure 3. Photoluminescence spectra of samples (a) of CaO doped with Sm<sup>3+</sup> and co-doped with Li<sup>+</sup>,Na<sup>+</sup>, K<sup>+</sup> and (b) CaO:Sm<sup>3+</sup>, SrO:Sm<sup>3+</sup> and CaSrO<sub>2</sub>:Sm<sup>3+</sup>.

With the introduction of alkali metal ions, M<sup>+</sup> (M<sup>+</sup> = Li<sup>+</sup>, Na<sup>+</sup>, K<sup>+</sup>) in the CaO:Sm<sup>3+</sup> system we observed a remarkable enhancement of luminescence of all emission peaks from  $\mathrm{Sm}^{3+}$  particularly for  ${}^{4}\mathrm{G}_{5/2} \rightarrow {}^{6}\mathrm{H}_{5/2}$ ,  $^4G_{5/2} \rightarrow ^6H_{7/2} \& ^4G_{5/2} \rightarrow ^6H_{9/2}$  transition (Fig. 3). There is an increase of about 20, 30 and 500 % respectively in the luminescence intensity when Na<sup>+</sup>, Li<sup>+</sup> and K<sup>+</sup> ions are doped. It seems that the incorporation of mono-valent ions facilitate the improved energy transfer from Ca<sup>2+</sup> to Sm<sup>3+</sup> and creating the oxygen vacancies. As a result, these oxygen vacancies, which may act as sensitizers, facilitate the strong mixing of the Ca-O and Sm-O charge transfer states, and thus promote energy migration from the Ca-O CTS(charge transfer state ) to Sm<sup>3+</sup>. In a similar case [13], the enhancement of Sm<sup>3+</sup> luminescence intensity with the co-doping of alkali metals ions in Sr<sub>2</sub>CeO<sub>4</sub> host lattice is due to the generation of oxygen vacancies to promote the energy transfer from Ce<sup>4+</sup> to Sm3+, reduce environment symmetry around Sm3+ ions and cause hole traps to quench the CeO CTS luminescence. Furthermore, more are the oxygen vacancies generated by doping ions, more is the effective energy transfer between Ca<sup>2+</sup> and Sm<sup>3+</sup> ions. Finally, it can be concluded that the large increase in the emission intensity of the  ${}^4G_{5/2} \rightarrow {}^6H_{1/2}$  (J= 5,7,9) transitions is due to improved energy transfer and reduced symmetrical environment around Sm<sup>3+</sup>. Alkali-metals ions co-doping had different effects on energy transfer (K<sup>+</sup> > Li<sup>+</sup> > Na<sup>+</sup>), which is in accordance with the sequence of luminescence from  ${}^4G_{5/2} \rightarrow {}^6H_{J/2}$  (J= 5,7,9) transition of the  $Sm^{3+}$ .

#### VI. CONCLUSION

CaO:Sm<sup>3+</sup>, M<sup>+</sup> (Li<sup>+</sup>, Na<sup>+</sup>, K<sup>+</sup>), SrO:Sm<sup>3+</sup> and CaSrO<sub>2</sub>:Sm<sup>3+</sup> powders prepared by combustion synthesis method and further heating to  $1000\,^{\circ}$ C improved the crystallanity of the materials. XRD analysis showed that cubic phase is mainly present in CaO:Sm<sup>3+</sup>,M<sup>+</sup> (Li<sup>+</sup>, Na<sup>+</sup>, K<sup>+</sup>) samples; tetragonal in SrO and monoclinic in Sm<sub>2</sub>O<sub>3</sub> are the main phases in the SrO:Sm<sup>3+</sup> and CaSrO<sub>2</sub>:Sm<sup>3+</sup> powders. A remarkable increase in the photoluminescence intensity by co-doping with alkali metal ions in CaO:Sm<sup>3+</sup> is due to the generation of oxygen vacancies to promote energy transfer from Ca<sup>2+</sup> to Sm<sup>3+</sup> and reduce environment symmetry around Sm<sup>3+</sup> ions.

#### **REFERENCES**

- [1] Y. Ding, F.R. Fan, Z.Q. Tian, and Z.L. Wang, J. Am. Chem. Soc., 132, 2010, 12480.
- [2] W. Feng, 2. L.D. Sun, Y.W. Zhang, and C.H. Yan, Coord. Chem. Rev., 254, 2010, 1038.

Vol. No.6, Issue No. 01, January 2017

## www.ijarse.com

- IJARSE ISSN (O) 2319 - 8354 ISSN (P) 2319 - 8346
- [3] W.B. Bu, Y.P. Xu, 3. N. Zhang, H.R. Chen, Z.L. Hua, and J.L. Shi, Langmuir, 23, 2007, 9002.
- [4] I. Park, Y. Kima, and D. J. Lee, J Mater Chem Phys, 106, 2007,149.
- [5] W. Di, X. Zhao, and S. Lu, J Solid State Chem, 180, 2007, 2478.
- [6] D. Uhlich, P. Huppertz, D.U. Wiechert, and T. Justel, J Opt Mater, 29, 2007, 1505.
- [7] M. Kang, X.Liao, Y. Kang, J. Liu, R. Sun, G. Yin, Z. Huan, and Y. Yao, J. Mater. Sci.,44, 2009, 2388.
- [8] A.G. Joly, W. Chen, J. Zhang, and S. Wang, J. Lumin, 126, 2007, 491.
- [9] Y. Conga, B. Lia, B. Leia, X. Wanga, C. Liua, J. Liua, W. Li, J Lumin, 128, 2008, 105.
- [10] X. Xiao and B.J. Yan, Mater Lett, 61, 2007, 1649.
- [11] J. H. Jeong, H. K. Yang, and K.S. Shim, Appl Surf Sci, 253, 2007, 8273.
- [12] J. Fu (2000) J Electron Solid-State Lett 3,350
- [13] D.V. Voort, A. Imhof, and G. Blasse, J. Solid State Chem. 96, 1992, 311.
- [14] Li Shi Li, Yu Li Cheng, and Su. Qiang, J.fluorescence, 21, 2011, 1461.
- [15] G. Liu, G. Hong, J. Wang, and X. Dong, J. Alloys Compd, 432, 2007, 200.
- [16] R.S. Ningthoujam, V. Sudarsan, and S. K. Kulshreshtha, J. Lumin, 127, 2007, 747.
- [17] X.R. Gao, L. X. Lei, Y.M. Sun, H.G. Zheng, and Y.P. Cui, J Solid State Chem, 181, 2008, 177.
- [18] X. Liu and X. Wang, Opt Mater, 30, 2007, 626.
- [19] L.C. Porter and J.C. Wright, J. Chem. Phys. 77, 1982, 2322.